

RESEARCH ARTICLE

10.1002/2015GC005805

Magmatic recharge in continental flood basalts: Insights from the Chifeng igneous province in Inner Mongolia

Xun Yu^{1,2}, Cin-Ty A. Lee², Li-Hui Chen¹, and Gang Zeng¹¹State Key Laboratory for Mineral Deposits Research, School of Earth Sciences and Engineering, Nanjing University, Nanjing, China, ²Department of Earth Science, MS-126 Rice University, Houston, Texas, USA

Key Points:

- Increasing primitiveness is common in flood basalts
- Increasing primitiveness is caused by magmatic recharge
- History of magma chambers revealed by continuous basalt stratigraphy

Correspondence to:

X. Yu,
yuxun.nju@hotmail.com

Citation:

Yu, X., C.-T. A. Lee, L.-H. Chen, and G. Zeng (2015), Magmatic recharge in continental flood basalts: Insights from the Chifeng igneous province in Inner Mongolia, *Geochem. Geophys. Geosyst.*, 16, 2082–2096, doi:10.1002/2015GC005805.

Received 9 MAR 2015

Accepted 4 JUN 2015

Accepted article online 9 JUN 2015

Published online 6 JUL 2015

Abstract Eruptive sequences can be used as windows into the thermal and chemical evolution of magma chambers. We examined a continuous vertical section of the Baichahe basalt flow associated with the late Cenozoic Chifeng flood basalt in Inner Mongolia, North China. From oldest to youngest, MgO increases, K₂O, light rare earths and other incompatible elements decrease, and Nb/La and radiogenic Pb isotopic ratios increase, all of which indicate increasing primitiveness and decreasing contribution of crustal contamination with time. The variable Pb isotope and incompatible element ratios require a component of crustal contamination, most likely of the lower crust (unradiogenic Pb, and low Ce/Pb), in the earliest lavas. Fractional crystallization can explain some of the elemental systematics, but alone cannot explain variable incompatible element ratios and Pb isotopes, nor the temporal trend to more primitive compositions. Crustal assimilation with or without fractional crystallization also cannot explain all the elemental systematics. We find instead that recharge by a primitive magma, in combination with fractional crystallization and decreasing rates of crustal assimilation, is needed to explain the observed geochemical systematics. Our observations suggest that the delivery of fresh basalt to the magma chamber must increase at rates faster than the crust can be assimilated or that the rates of crustal assimilation must decrease. However, progressive addition of primitive magma should heat up the crust and lead to more crustal assimilation. We suggest that during the initial stages of forming a magma chamber, the magma cools and develops an outer crystalline rind of mafic to ultramafic cumulates. This results in a thickening nonconvecting chemical boundary layer, which serves to insulate the magma chamber from further assimilation of crust and cooling, the latter resulting in the reduction of crystallization rates and the buffering of magma compositions at more primitive compositions. We show that certain segments of other large igneous provinces also display an evolution toward more primitive magmas with time, indicating that magmatic recharge may be a common feature of basaltic magma chambers.

1. Introduction

Flood basalts are massive outpourings of basalts over a narrow window of time, and because of their impact on continent formation and climate, their origins are of interest and debate [e.g., Ali *et al.*, 2005; Lassiter and DePaolo, 1997; Lightfoot and Hawkesworth, 1988; Sharma, 1997; White and McKenzie, 1995]. Although it is generally agreed that flood basalts derive from the mantle, it is not clear whether they derive by decompression melting in high-temperature plumes, decompression melting driven by lithospheric extension or melting of fertile lithologies in the mantle at otherwise normal temperatures [e.g., Anderson, 1994; King and Anderson, 1995; Silver *et al.*, 2006; White and McKenzie, 1995]. The geochemical composition of magmas can be used to infer the nature of the mantle source of flood basalts, allowing one to evaluate source fertility, mantle temperature, timing of emplacement, etc. However, magma chamber processes pose a complicating factor. As primitive magmas depart from the mantle and intrude into the cold crust, they may pool as magma chambers, cool and crystallize, assimilate country rock, and erupt. Effects of lithospheric contamination can be pronounced, at least chemically and isotopically for continental flood basalts [e.g., Arndt *et al.*, 1993; Carlson *et al.*, 1981]. Finally, magma chambers that serve as intermediate staging zones that feed the flood basalts likely experience periodic or continuous recharge of primitive magma. Clearly, flood basalts represent complex blends of crustal melts, residual magmas, and recharging parental magmas [e.g., Lightfoot *et al.*, 1990; Sharma *et al.*, 1991; Wooden *et al.*, 1993]. The purpose of this study is to better understand how these different magma chamber processes influence the composition of flood basalts.

One way to gain insight into how magma chambers evolve is to investigate the “stratigraphy” of continuous lava flows in flood basalt provinces. As a case study, we investigated a late Cenozoic sequence of flows associated with the Chifeng continental flood basalt erupted in Inner Mongolia in northern China [Han *et al.*, 1999; Ho *et al.*, 2008; Hong *et al.*, 2013; Jia *et al.*, 2002]. The earliest lavas are more evolved and show greater extents of crustal assimilation while subsequent lavas become more primitive with time. We discuss the origin of this trend toward increasing primitiveness in the context of recharge, eruption, assimilation, and fractional crystallization. We show that trends or cycles of increasing primitiveness are seen in other continental flood basalt sequences, suggesting that magmatic recharge may be a common mechanism in the formation of flood basalts.

2. Geological Background and Sample Descriptions

The Chifeng flood basalt field (CFB) lies on the north edge of North China Craton (Figure 1a) and represents part of a 20,000 km² Neogene flood basalt belt [Chen *et al.*, 2014; Han *et al.*, 1999; Liu *et al.*, 1992]. The basalt is composed of several hundred meters of flow overlain by Quaternary sediments [Han *et al.*, 1999]. Cenozoic eruptions in the Chifeng area young gradually from the southeast to the northwest. According to Jia *et al.* [2002], the CFB basalts can be divided into four stages: a <200 m Oligocene (33–24 Ma) stage in the southeastern part of the CFB, a <400 m late Miocene flow interval (10–6 Ma) in the central part of the CFB, a <100 m Pliocene flow interval (~5 Ma) in the north [Jia *et al.*, 2002], and a Pleistocene flow interval (0.89–0.16 Ma) as scattered outcrops in the northwest [Hong *et al.*, 2013; Jia *et al.*, 2002]. These flood basalts are likely related to the opening of the Bohai basin to the southeast and associated lithospheric extension [Han *et al.*, 1999; Hu *et al.*, 2001].

Here we investigated a Pliocene vertical section (E117°57'58.16", N43°06'52.00") known as the Baichahe group (Figure 1a). The eruptions produced a series of layered basalts as thick as 40–70 m [Jia *et al.*, 2002]. The section consists of at least 10 individual lava flows, identified by the presence of paleo flow surfaces. The lava layers are thought to be relatively continuous because no soil or sediments were found between them, suggesting that this sequence was erupted in a short time interval [Jia *et al.*, 2002]. We obtained fresh samples from nine consecutive flows, totaling 40 m. The total thickness of the top three layers is similar to the total thickness of the middle three layers which are greater than 15 m, while the thickness of the bottom three layers is less than 10 meters (Figures 1b and 1c). In hand sample, the basalts are black and massive and contain a few small (<1 cm) felsic xenoliths. The basalts exhibit porphyritic to aphyric textures with olivine and clinopyroxene phenocrysts set within groundmass composed of fine to medium-grained plagioclase, clinopyroxene, olivine, and Fe-Ti oxides.

3. Methods

Measurements of whole-rock major elements were made at the State Key Laboratory for Mineral Deposits Research, Nanjing University, China, using a Thermo Scientific ARL 9900 X-ray fluorescence spectrometer (XRF). According to the measured values of standards (GSR-1 and GSR-3), the relative standard deviation is about ±1% for elements with concentrations >1.0 wt %, and about ±10% for the elements with concentrations <1.0 wt %. Measurements of whole-rock trace elements were made at the Department of Geology, Northwest University, China. Trace elements, including the rare earth elements (REEs), were determined using an ELANG100DRC inductively coupled plasma mass spectrometer (ICP-MS) after acid digestion of samples in Teflon bombs. Analyses of the USGS rock standards (BHVO-2, AGV-2, BCR-2, and GSP-1) indicate precision and accuracy better than 5% for Sc, V, Co, Zn, Rb, Sr, Y, Nb, Cs, Ba, Th, and REEs, and 10% for Li, Cu, Zr, Hf, Ta, Pb, and U.

Pb isotopic compositions were obtained using a Neptune plus (Thermo Fisher Scientific) multicollector inductively coupled plasma mass spectrometer (MC-ICP-MS) at the State Key Laboratory for Mineral Deposits Research in Nanjing University, China. Approximately 200 mg powders were leached for 12 h in warm 2.5 N HCl before dissolving in an HF-HNO₃ acid mixture at 120°C for more than 36 h. After evaporation to dryness, all samples were repeatedly taken up and dried with concentrated HNO₃ with traces of HF in order to break CaF bonds. Finally, the samples were dissolved in HBr-HNO₃ acid mixture. Pb was separated from the rock matrix by chromatographic extraction using an anion exchange resin (200–400 mesh Bio-RAD resin). Detailed chemical separation procedures are given by Kuritani and Nakamura [2002]. Thallium was

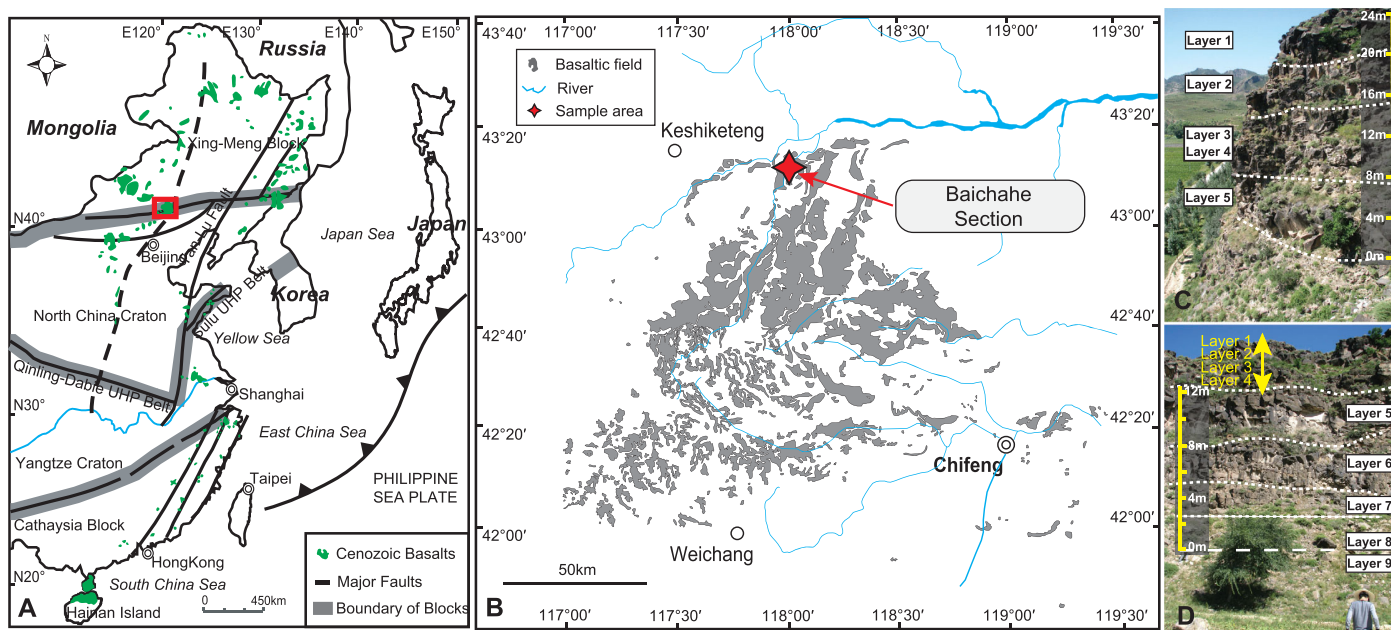


Figure 1. (a) Simplified geological map of eastern China and (b) distribution of Cenozoic basalts in Chifeng area. (c) Top five layers of Baichahe vertical section. (d) Bottom four layers of Baichahe vertical section.

added to correct for mass bias during the measurement. Measured Pb isotopic ratios were corrected for instrumental mass fractionation by reference to replicate analyses of the standard NIST-981. Detailed measurement procedures are given by *White et al.* [2000]. Measured values for NIST-981 are 16.9396 ± 7 (2SE) for $^{206}\text{Pb}/^{204}\text{Pb}$, 15.4855 ± 7 (2SE) for $^{207}\text{Pb}/^{204}\text{Pb}$, and 36.6874 ± 16 (2SE) for $^{208}\text{Pb}/^{204}\text{Pb}$, respectively. The results of the analyses of samples can be seen in Table 1.

4. Results

Samples from the Baichahe section are alkaline basalt (mainly trachy-basalt): they have moderate SiO_2 (47.4–48.7 wt %) and high alkalis ($\text{Na}_2\text{O} + \text{K}_2\text{O} = 5.0\text{--}6.5$ wt %). MgO increases and K_2O decreases up section, indicating a trend toward more primitive compositions with younging age. Crust-sensitive tracers also decrease up section. Incompatible elements like Nb and La decrease. Nb/La and Ce/Pb, which are generally low in continental crust, increase up section. Lead isotopic ratios $^{206}\text{Pb}/^{204}\text{Pb}$, $^{207}\text{Pb}/^{204}\text{Pb}$, and $^{208}\text{Pb}/^{204}\text{Pb}$ increase up section from unradiogenic values more similar to those of lower continental crust from the North China craton [*Liu et al.*, 2004] (Figure 2). The increasing primitiveness and decreasing crustal contribution up section can also be seen in primitive mantle-normalized trace element diagrams: basalts from lower layers show stronger relative enrichments of incompatible to moderately incompatible elements, as can be seen from the higher light rare earth element enrichment signatures of the lower layers compared to the upper layers (Figure 3).

5. Discussion

5.1. Increasing Primitiveness of Magma

The geochemical and isotopic trends described above indicate that magmas become increasingly primitive with time. These geochemical trends also translate into temperature. Liquid temperatures of each layer scale with whole-rock MgO contents if olivine is present. Using the thermometry of *Lee and Chin* [2014] and assuming that the magmas were dry and resided in a midcrustal magma chamber (a pressure of 0.5 GPa was assumed), we estimate liquid temperatures to vary from 1220 to 1263°C up section (Figure 2). These temperatures represent the temperature of the magma body at the time each layer was erupted. There may be some absolute uncertainties in the temperatures but the relative variations are likely robust.

Table 1. Geochemical Compositions of Baichahe Layered Basalts

Analysis No.	Layer 1 (Top) 11BCH01	Layer 2 11BCH02	Layer 3 11BCH03	Layer 4 11BCH04	Layer 5 11BCH05	Layer 6 11BCH06	Layer 7 11BCH07	Layer 8 11BCH08	Layer 9 (Bottom) 11BCH09	This Study BHVO-2	This Reference ^a BHVO-2	This Study AGV-2	This Reference AGV-2	This Study BCR-2	This Reference BCR-2	This Study GSP-1	This Reference GSP-1
<i>Major Element (wt %)</i>																	
SiO ₂	47.6	47.68	47.8	47.39	47.8	48.28	48.74	48.54	48.3								
TiO ₂	2.068	2.071	2.148	2.197	2.17	2.234	2.345	2.254	2.257								
Al ₂ O ₃	12.64	12.11	12.71	13.46	13.94	13.84	14.52	13.91	14.04								
Fe ₂ O ₃ T ^b	12.34	12.2	12.17	11.79	12.04	11.98	11.45	11.84	11.57								
MnO	0.156	0.152	0.153	0.146	0.151	0.148	0.139	0.152	0.153								
MgO	10.55	10.39	10.02	8.6	8.3	8.49	7.7	8.73	8.48								
CaO	8.54	9.52	8.8	9.18	8.73	8.51	8.02	7.94	8								
Na ₂ O	3.95	3.42	3.81	4.12	3.76	3.98	4.4	4.06	3.71								
K ₂ O	1.69	1.57	1.68	1.81	1.74	1.81	2.13	2.03	2.08								
P ₂ O ₅	0.492	0.5	0.508	0.551	0.552	0.563	0.617	0.598	0.615								
LOI	0.04	0.22	0.17	0.89	0.96	0.12	0	0.06	0.41								
TOTAL	100.06	99.84	99.97	100.13	100.15	99.95	100.06	100.12	99.61								
<i>Trace Element (ppm)</i>																	
Li	9.10	9.86	8.15	7.86	11.5	8.04	8.12	9.19	10.8	4.79	4.80	11.0	11.0	9.46	9.00	30.6	31.0
Be	1.74	1.58	1.77	1.84	1.85	1.89	2.11	2.04	2.00	1.06	1.00	2.21	2.30	2.09	1.60	1.27	1.40
Sc	19.6	23.3	20.3	17.1	16.9	17.6	16.0	16.8	16.8	32.2	32.0	12.6	13.0	34.5	33.0	6.45	6.20
V	185	203	189	177	177	183	178	179	176	320	317	117	120	414	416	52.8	53.0
Cr	316	461	319	205	182	217	151	207	201	284	280	15.4	17.0	15.6	18.0	9.88	13.0
Co	59.2	56.7	55.3	50.6	52.5	51.3	46.3	51.1	48.8	45.9	45.0	15.4	16.0	38.4	37.0	6.75	6.60
Ni	286	269	254	218	218	220	187	227	217	120	119	18.5	20.0	12.2	13.0	7.17	8.80
Cu	53.3	49.1	55.6	57.5	51.7	57.8	59.3	54.0	52.6	130	127	48.9	53.0	20.9	21.0	30.4	33.0
Zn	113	105	108	109	111	111	111	111	111	102	103	86.3	86.0	128	127	100	104
Ga	19.5	18.4	19.0	20.2	20.4	20.8	22.0	21.0	21.3	21.5	21.7	20.3	20.0	21.7	23.0	26.0	23.0
Ge	1.35	1.36	1.30	1.28	1.30	1.32	1.31	1.30	1.35	1.60	1.60	1.16		1.56		1.87	1.36
Rb	23.5	20.4	22.6	23.9	22.4	24.1	31.1	27.4	28.9	9.06	9.11	66.34	66.30	46.99	46.90	241.09	254.00
Sr	690	538	665	585	627	605	670	645	667	399	396	659	661	340	340	229	234
Y	20.9	20.3	20.6	21.7	21.4	22.0	23.3	22.6	23.2	26.4	26.0	19.8	20.0	36.1	37.0	27.1	26.0
Zr	175	162	171	181	177	186	210	200	206	171	172	231	230	186	184	586	530
Nb	39.9	36.3	39.1	42.2	40.6	43.2	48.3	45.9	46.6	18.6	18.1	14.1	14.5	12.6	12.6	29.1	27.9
Cs	0.41	0.34	0.37	0.37	0.25	0.35	0.46	0.38	0.44	0.11	0.10	1.14	1.16	1.13	1.10	0.98	1.02
Ba	287	269	337	312	374	339	378	352	393	128	131	1134	1130	678	677	1285	1310
La	22.6	20.5	21.7	23.5	23.5	24.3	28.1	26.8	28.0	15.0	15.2	38.2	37.9	24.0	24.9	175.7	184.0
Ce	46.4	42.4	44.5	48.3	47.2	49.6	57.3	54.5	57.2	37.9	37.5	68.3	68.6	52.3	52.9	416.1	399.0
Pr	5.72	5.26	5.47	5.91	5.82	6.10	6.95	6.68	6.94	5.26	5.35	8.01	7.84	6.63	6.70	55.64	52.00
Nd	24.0	22.4	23.1	24.9	24.5	25.5	28.5	27.5	28.6	24.8	24.5	30.3	30.5	28.2	28.7	207.2	196.0
Sm	5.64	5.39	5.50	5.79	5.68	5.95	6.44	6.28	6.43	6.13	6.07	5.47	5.49	6.47	6.58	25.4	26.3
Eu	1.81	1.76	1.78	1.86	1.88	1.92	2.08	2.02	2.07	2.08	2.07	1.56	1.54	1.94	1.96	2.25	2.33
Gd	5.21	4.97	5.04	5.34	5.27	5.51	5.91	5.71	5.87	6.05	6.24	4.67	4.52	6.40	6.75	14.5	12.1
Tb	0.78	0.75	0.76	0.80	0.78	0.81	0.87	0.84	0.85	0.93	0.92	0.63	0.64	1.02	1.07	1.38	1.34
Dy	4.23	4.13	4.12	4.34	4.28	4.45	4.77	4.54	4.68	5.31	5.31	3.47	3.47	6.25	6.41	6.23	5.50
Ho	0.75	0.73	0.72	0.76	0.76	0.79	0.83	0.80	0.83	0.98	0.98	0.65	0.65	1.26	1.28	0.94	1.01
Er	1.91	1.79	1.81	1.91	1.88	1.98	2.12	2.02	2.07	2.55	2.54	1.82	1.81	3.59	3.66	2.50	2.70
Tm	0.24	0.23	0.23	0.25	0.25	0.26	0.27	0.26	0.27	0.33	0.33	0.25	0.26	0.51	0.54	0.29	0.38
Yb	1.42	1.33	1.34	1.43	1.40	1.47	1.56	1.50	1.55	2.01	2.00	1.62	1.62	3.32	3.38	1.67	1.70
Lu	0.19	0.18	0.19	0.20	0.19	0.20	0.21	0.21	0.21	0.28	0.27	0.24	0.25	0.49	0.50	0.24	0.21
Hf	3.93	3.70	3.79	4.02	3.94	4.16	4.61	4.39	4.53	4.38	4.36	5.03	5.00	4.73	4.90	14.6	15.5
Ta	2.15	1.98	2.10	2.29	2.19	2.33	2.60	2.49	2.55	1.18	1.14	0.84	0.87	0.77	0.78	0.89	0.97
Pb	2.91	2.38	2.48	2.73	2.57	2.92	3.67	3.50	3.86	1.67	1.60	13.1	13.2	10.1	11.0	59.5	55.0
Th	3.18	2.81	3.01	3.28	3.19	3.40	4.09	3.92	4.11	1.23	1.22	6.05	6.10	5.77	5.70	106	106
U	0.95	0.74	0.95	1.00	1.04	1.01	1.20	1.16	1.23	0.42	0.40	1.84	1.86	1.62	1.69	2.34	2.54
<i>Isotope</i>																	
²⁰⁶ Pb/ ²⁰⁴ Pb	18.0064	18.0345	18.0323	18.0164	18.012	18.0161	17.9536	17.9476	17.9348								
2SE ^c	0.0006	0.0007	0.0007	0.0007	0.0012	0.0006	0.0005	0.0006	0.0007								
²⁰⁷ Pb/ ²⁰⁴ Pb	15.4848	15.495	15.4986	15.4818	15.4845	15.504	15.4764	15.4751	15.4758								
2SE	0.0006	0.0008	0.0006	0.0006	0.0011	0.0005	0.0004	0.0005	0.0007								
²⁰⁸ Pb/ ²⁰⁴ Pb	38.0448	38.0843	38.0812	38.0478	38.058	38.0867	38.0059	38.0023	38.0047								
2SE	0.0015	0.0022	0.0017	0.0017	0.0026	0.0014	0.0012	0.0014	0.0017								
Ce/Pb	15.95	17.85	17.97	17.71	18.37	17.00	15.64	15.56	14.82								
Nb/La	1.77	1.77	1.80	1.79	1.73	1.78	1.72	1.71	1.66								
Tm(°C) ^d	1263	1260	1255	1234	1229	1232	1220	1236	1232								

^aReference data for BHVO-2, AGV-2, BCR-2, and GSP-1 are taken from Govindaraju [1994].

^bFe₂O₃T, total iron as Fe₂O₃.

^cSE refers to standard error.

^dLiquid temperatures for lavas from different layers [Lee and Chin, 2014]. Here we assumed H₂O = 0 wt %, and P = 0.5 Gpa.

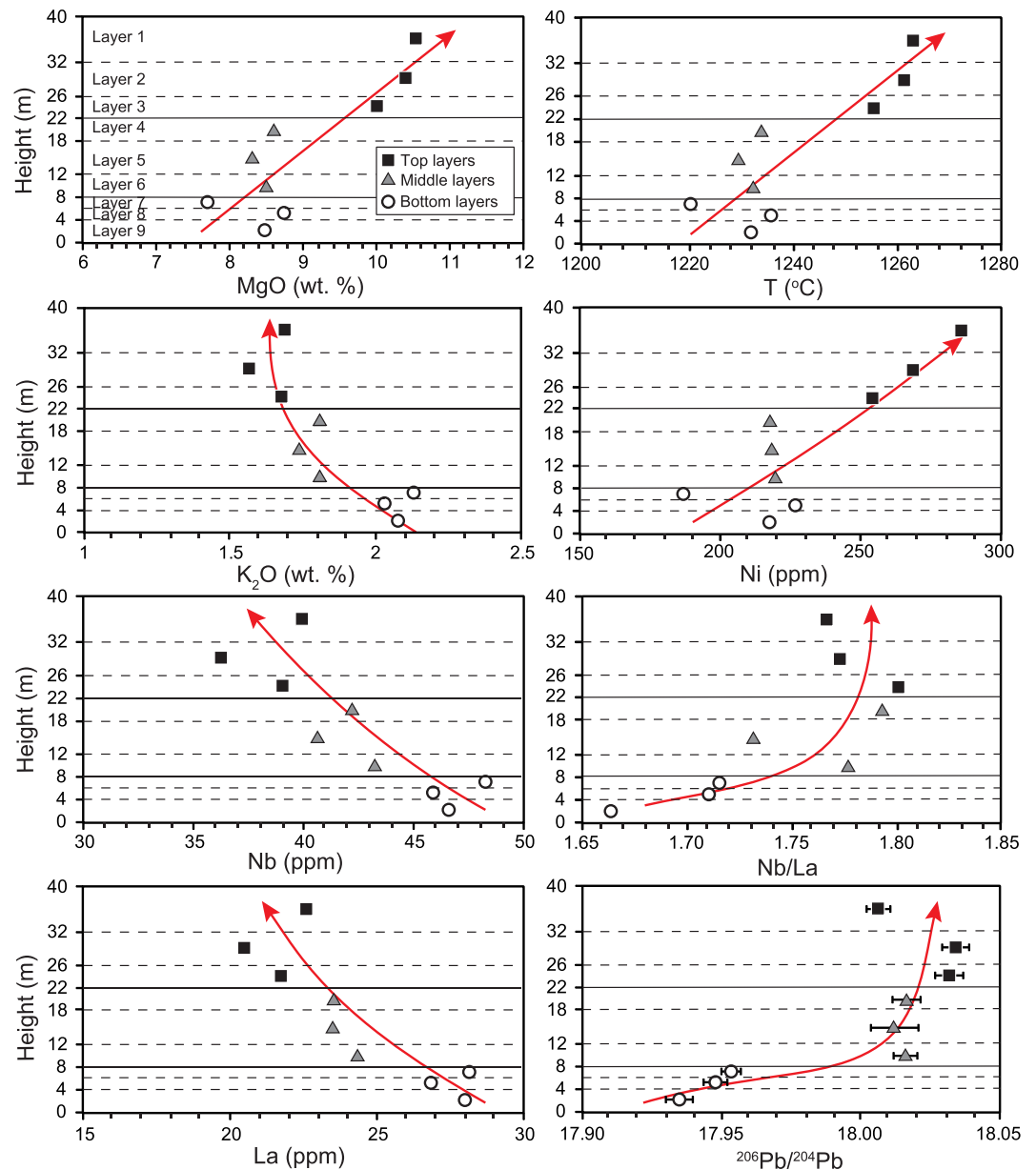


Figure 2. Spatial variations for representative major, trace elements, and isotopes. Vertical axis shows the heights of vertical section. Horizontal axis shows variations of wt % MgO and K₂O, ppm Nb, La, and Ni, Nb/La, ²⁰⁶Pb/²⁰⁴Pb and the temperature (°C) of magma. Dotted and straight curves represent the boundaries of different layers.

Collectively, our observations indicate that the magma chamber became more primitive, hotter, and assimilated less crustal wall rock with time.

Increasing primitiveness with time can be explained by a change in the nature of mantle source or by magma chamber processes. For example, variations in flood basalt sequences are commonly explained by early melting of enriched mantle components and later melting of less enriched components [e.g., *Lassiter et al., 1995; Lassiter and DePaolo, 1997; Wooden et al., 1993*]. However, we note that the 1220–1263°C liquid temperatures calculated for the basaltic lavas are well below primary mantle-derived magma temperatures, indicating that the effects of magmatic differentiation in the crust must be considered. Below, we thus explore whether the compositional trends displayed in the Chifeng series can be explained by magma chamber processes.

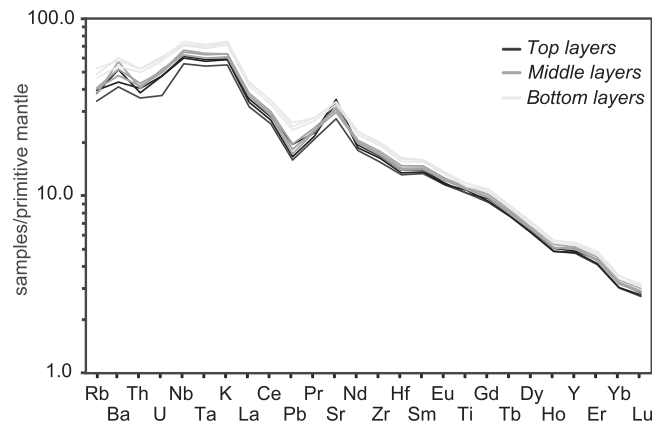


Figure 3. Primitive mantle-normalized trace element diagram of basalts from Baichahe vertical section. Primitive mantle values are from *McDonough and Sun* [1995].

5.2. Simultaneous Recharge, Eruption, Assimilation, and Fractional Crystallization (REAFC)

The processes that influence the compositional evolution of a magma chamber are magma recharge (R), crustal assimilation (A), fractional crystallization (FC), and eruption (E) [e.g., *DePaolo*, 1981; *Lee et al.*, 2014; *Spera and Bohrsen*, 2001, 2002]. For the Chifeng series, fractional crystallization (FC) alone cannot change Pb isotopes or incompatible element ratios like Nb/La and does not explain the increasing primitiveness with time (Figure 4). Similarly, crustal assimilation (A) alone does not match the observed data because

it predicts a decrease in Nb/La and radiogenic Pb isotopes with decreasing MgO content because the continental crust end-member is characterized by low Nb/La and unradiogenic Pb ($^{206}\text{Pb}/^{204}\text{Pb}$ in the crust of the North China craton are as low as 16.5) [*Gao et al.*, 1998; *Liu et al.*, 2004]; although Nb/La and $^{206}\text{Pb}/^{204}\text{Pb}$ are indeed low for the samples with the lowest MgO contents (<8 wt %), these ratios remain constant between 8 and 11 wt % MgO (Figure 4). Simultaneous assimilation and fractional crystallization (AFC) can potentially explain some of the elemental and isotopic trends, but cannot explain the increase in primitiveness with time (Figure 4). In summary, the increasing primitiveness of the magmas with time requires some component of recharge (R) by a primitive parental magma.

We now consider the relative importance of recharge, eruption, assimilation, and fractional crystallization (REAFC) on the Chifeng basalts. Different approaches can be explored. One approach is to follow the energy-constrained approach of *Spera and Bohrsen* [2004], wherein the amount of assimilation is limited by energy availability from the host magma itself and the efficiency of heating up the country rock. While such

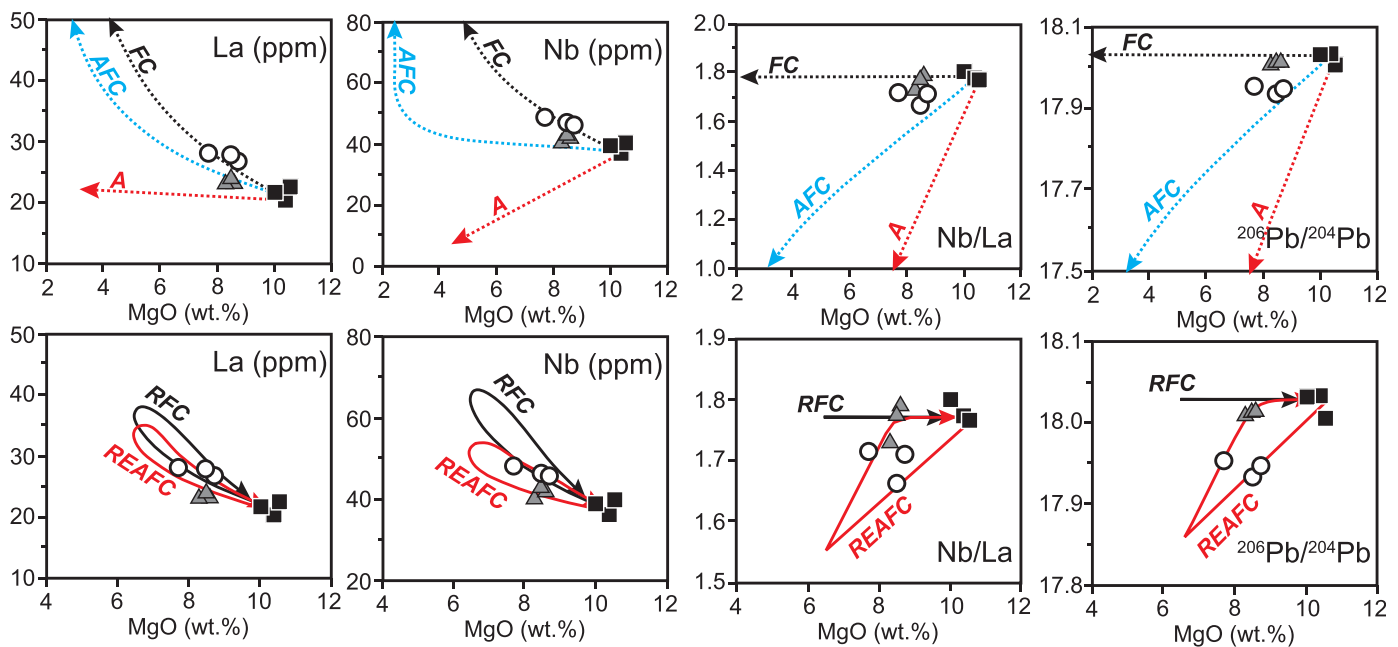


Figure 4. Modeling results of pure fractional crystallization with (black lines) or without recharge (black dotted lines), assimilation with (blue dotted lines) or without fractional crystallization (red dotted lines), and simultaneous recharge, eruption, assimilation, and fractional crystallization model (red lines) for Baichahe basalts. Rayleigh fractional crystallization equation [*Gast*, 1968; *Shaw*, 1970] and Recharge-Eruption-Assimilation-Fractional Crystallization models [*Lee et al.*, 2014] are used here. Symbols are the same as Figure 2.

a model is in theory more realistic because physics, in the sense of energy conservation, is considered, the physics of heat transport, magma mixing, and assimilation are not explicitly considered, and as such, these models may be too restrictive in terms of the variable space. We have thus chosen to relax the physical limitations and instead explore different combinations of R, E, A, and FC that might match the temporal evolution of composition following a box model approach of *Lee et al.* [2014]. Without initially worrying about physical and energetic limitations, we identify the family of REAFC scenarios that can best reproduce the observed Chifeng trends (Figure 4). We then evaluate the physical plausibility of such scenarios.

Following *Lee et al.* [2014], the rate at which the mass M of the magma chamber changes is given by

$$\frac{dM}{dt} = \frac{dM_{re}}{dt} + \frac{dM_e}{dt} + \frac{dM_{cc}}{dt} + \frac{dM_x}{dt} \quad (1)$$

where the rates of recharge (R), eruption (E), assimilation (A), and fractional crystallization (FC) are dM_{re}/dt , dM_e/dt , dM_{cc}/dt , and dM_x/dt . Eruption and fractional crystallization rates are negative quantities because mass is removed from the magma chamber while recharge and assimilation are positive quantities because mass is added. Elemental mass balance is then given by

$$dm_{ch} = dM_x C_x + dM_e C_{ch} + dM_{cc} C_{cc} + dM_{re} C_{re} \quad (2)$$

where dm_{ch} is the change in mass of a given element in the magma chamber. C_{ch} , C_x , C_{cc} , C_{re} are the concentrations of the element in the magma chamber, crystallized minerals, crustal wall rock, and recharging magmas. C_x is related to the concentration in the residual liquid in the magma chamber C_{ch} by an equilibrium partition coefficient between crystals and melt, $D \equiv C_x/C_{ch}$. The actual composition of the recharging magma is not known, so we assume that the recharging magma is represented by the most primitive magma sampled in this study ($C_{MgO} = 10.5$ wt %, $C_{La} = 20.8$ ppm, $C_{Nb} = 37.0$ ppm, $C_{Pb} = 2.50$ ppm, $^{206}Pb/^{204}Pb = 18.03$). We also assume that the crystallizing phases are olivine and clinopyroxene with a ratio of ~ 1 . We thus adopt bulk partition coefficients for Mg, Nb, La, and Pb as $D_{Mg} \sim 2$, $D_{Nb} \sim 0.03$, $D_{La} \sim 0.028$, and $D_{Pb} \sim 0.001$ based on *McKenzie and O'Nions* [1991] and *O'Neill and Jenner* [2012], although the exact values of partition coefficients are not critical because we are only interested in general behaviors with these box models. Compositions of the lower continental crust from North China Craton are selected from *Gao et al.* [1998] ($C_{MgO} = 4.8$ wt %, $C_{La} = 20.0$ ppm, $C_{Nb} = 8.00$ ppm, $C_{Pb} = 15.0$ ppm, $^{206}Pb/^{204}Pb = 17.00$).

Below, we present the results of numerical models using equations (1) and (2) for different scenarios. In all models, we have normalized the mass of the magma chamber and all mass inputs and outputs to the initial mass of the magma chamber. Thus, the mass of the magma chamber initially is unity and the inputs and outputs effectively represent fractional quantities, that is, the proportion of mass added or removed relative to the original mass of the magma chamber. Because we do not have constraints on the lifespan of the magma chamber or actual mass inputs and outputs from the magma chamber, we use the integrated magmatic recharge mass $M_{re} = \int \frac{dM_{re}}{dt} dt$ as a progress variable instead of time, although M_{re} need not scale linearly with time. We then modify the ratios of the inputs and outputs relative to the recharge rate, which eliminates time as an explicit variable. Thus, we explore how the composition of the magma chamber varies as inputs and outputs, dM_i/dM_{re} , change with time or integrated magma chamber mass M_{re} . Although our approach treats all inputs and outputs as continuous, any stepwise changes in magma chemistry can be modeled as rapid changes in the magnitudes of certain inputs or outputs. We also assume that all magmas derive from the same magma chamber. Multiple magma chambers are possible but we have no reason to model such scenarios without any supporting or relevant data.

5.2.1. Nonsteady State Magma Chambers

Here we permit the magma chamber to change mass. We assume constant recharge rate dM_{re}/dt and vary one of the fluxes. In Figure 5a, we allow crystallization rates dM_x/dt to change while all other inputs, dM_{re}/dt , dM_e/dt , and dM_{cc}/dt , remain constant. When fractional crystallization increases faster than recharge, e.g., when dM_x/dM_{re} increases with time (line 1 in Figure 5a), magma compositions become depleted in Mg but more quickly contaminated by crustal components, as shown by rapid decreases in Nb/La and Pb isotopes compared to MgO decreases. When relative fractional crystallization rates dM_x/dM_{re} decrease with time (line 3 in Figure 5a), magma compositions initially become more evolved but eventually return to their primitive character in terms of elemental abundances. In this case, signatures of crustal assimilation in the form of

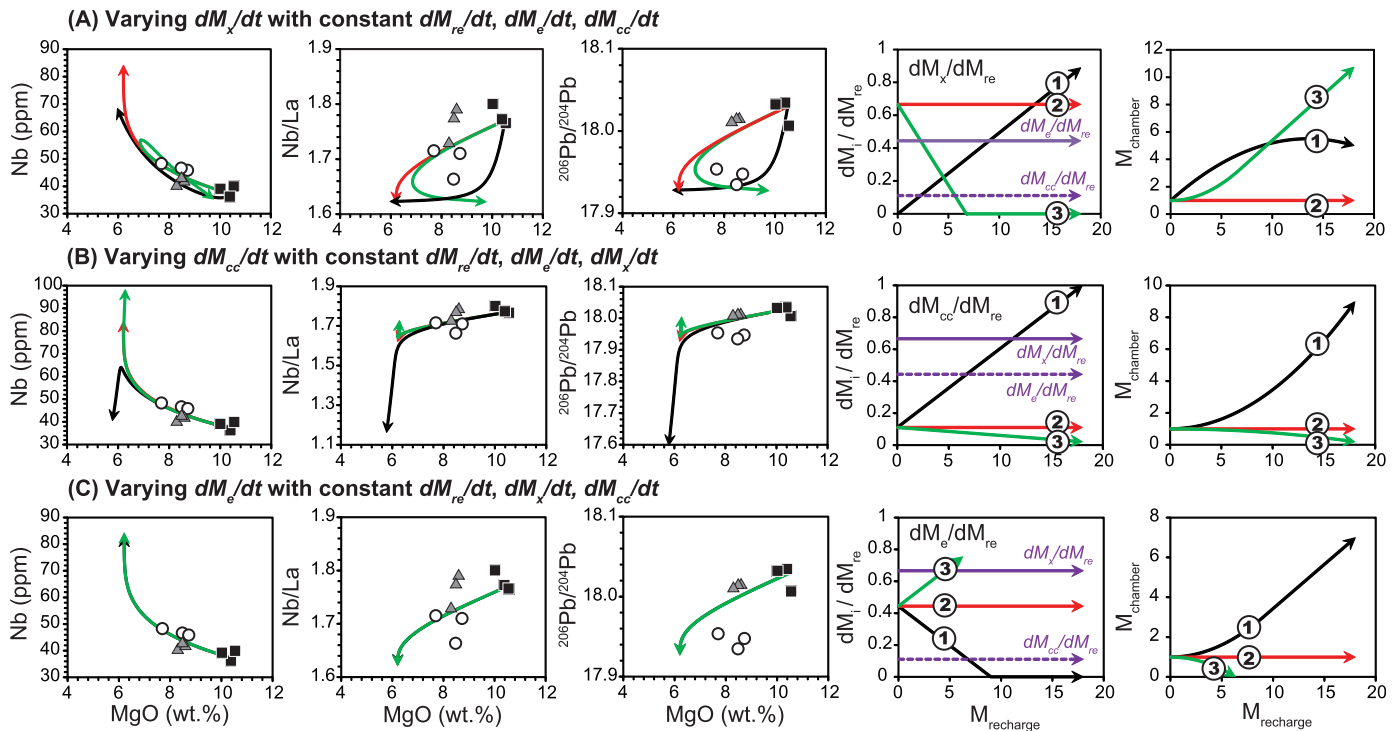


Figure 5. Effect of dM_{re}/dt , dM_e/dt , dM_{cc}/dt , and dM_x/dt on evolution of magma and mass of magma chamber. (a) Modeling results of variable fractional crystallization rates. Line 1 shows decreasing dM_x/dM_{re} while lines 2 and 3 show constant and increasing dM_x/dM_{re} . (b) Modeling results with variable assimilation rates. Line 1 shows increasing dM_{cc}/dM_{re} while lines 2 and 3 show constant and decreasing dM_{cc}/dM_{re} . (c) Modeling results with variable eruption rates. Line 1 shows decreasing dM_e/dM_{re} and lines 2 and 3 show constant and increasing dM_e/dM_{re} . REAFC models are assumed [Lee et al., 2014]. Symbols are the same as in Figure 2.

trace element and radiogenic isotope ratios (e.g., Nb/La or $^{206}\text{Pb}/^{204}\text{Pb}$) could be preserved even though major element systematics return to primitive compositions. This reflects the fact that the crustal trace element and isotopic signatures used here are fundamentally based on incompatible elements, which concentrate in the magma as the magma crystallizes. Thus, when the rate of fractional crystallization decreases relative to the rate of recharge, but crustal assimilation rates remain constant, the magma becomes more primitive in terms of major elements but can retain a signature of crustal contamination in terms of trace elements or radiogenic isotopes (line 3 in Figure 5a). Our data, however, show that crustal assimilation signatures decrease with increasing MgO content, suggesting that increasing recharge rates alone may not be sufficient.

In Figure 5b, we vary crustal assimilation dM_{cc}/dt , but hold all other fluxes, dM_{re}/dt , dM_e/dt , and dM_x/dt , constant. When relative crustal assimilation rates dM_{cc}/dM_{re} increase with time (line 1 in Figure 5b), the magma initially becomes more evolved with minimal effect of crustal assimilation, but eventually the magma develops continental crust-like elemental and isotopic signatures with little change in MgO content. When relative crustal assimilation rates dM_{cc}/dM_{re} decrease (line 3 in Figure 5b), the magma initially evolves to low Mg and high Nb contents, but gradually returns to its primitive character in terms of elemental and isotopic ratios, which can explain our observations.

In Figure 5c, we allow eruption rate dM_e/dt to change but hold dM_{re}/dt , dM_{cc}/dt , and dM_x/dt constant. Varying eruption rates, without changing any other relative fluxes, does not change elemental or isotopic variation diagrams. This is because it is assumed that erupted magmas have the same composition as the magma chamber. However, eruption strongly influences the rate at which magmas evolve because eruption decreases the size of the magma chamber, reducing the times for mixing and turnover. Thus, eruption alone cannot explain the return to primitive character of the magma with time.

5.2.2. Steady State Magma Chambers

We also consider a constant mass magma chamber ($dM_{ch}/dt = 0$) undergoing recharge (Figure 6). As shown above, decreasing fractional crystallization (dM_x/dM_{re}) and crustal assimilation rates (dM_{cc}/dM_{re}) relative to

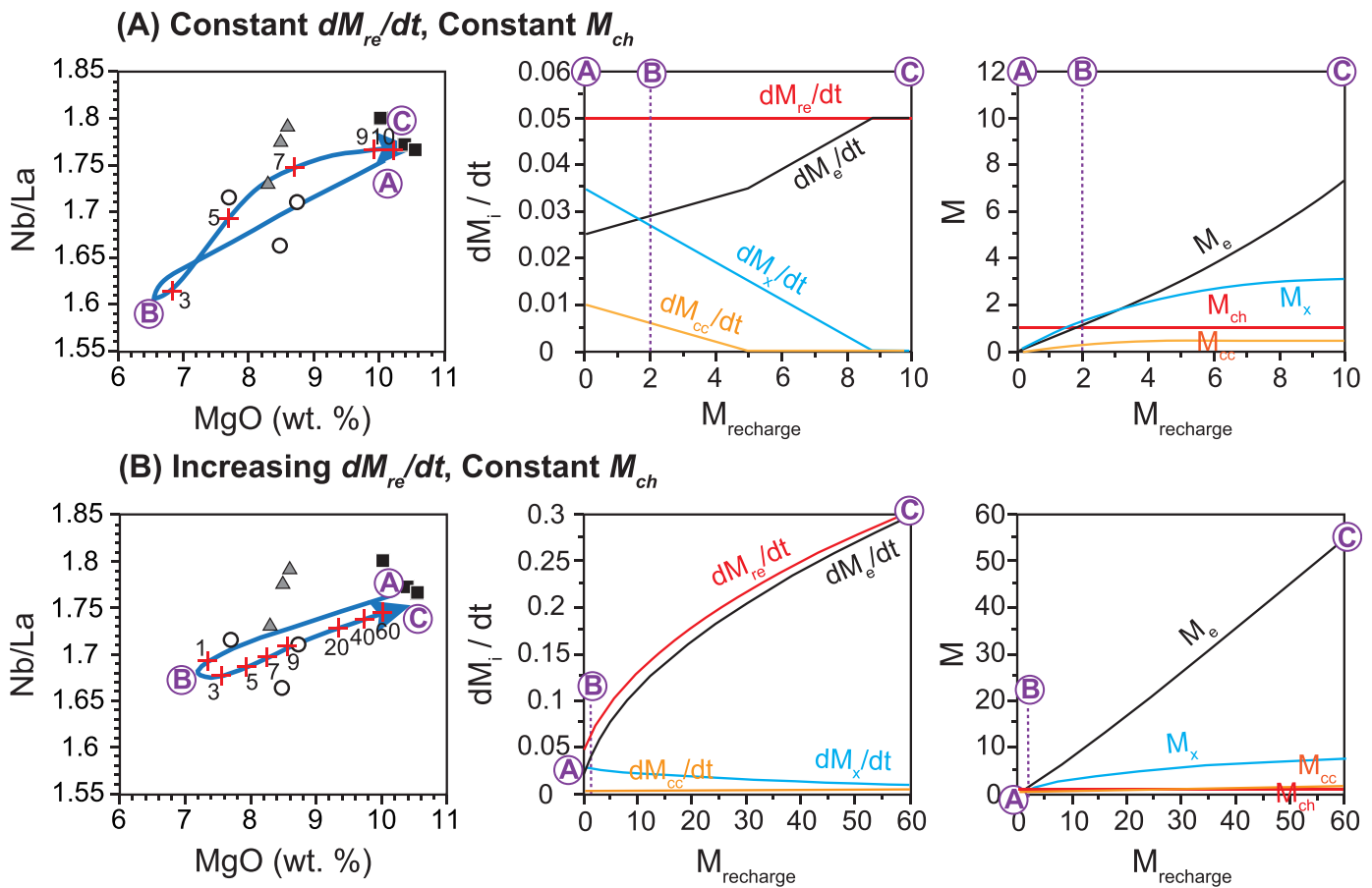


Figure 6. REAFC model results for constant mass magma chamber. (a) Decreasing assimilation rate. (b) Increasing assimilation rate. MgO and Nb/La are used in the modeling. Magma chamber is normalized to original mass. Tick marks on curves with labeled numbers represent overturn numbers. Symbols are the same as in Figure 2.

magmatic recharge rates is required for a magma to become more primitive and less crustally contaminated with time. For a constant mass magma chamber, we consider two extreme scenarios. In the first, the geochemical evolution of the magma chamber can be generated if we hold recharge rate dM_{re}/dt constant and allow crustal assimilation rate dM_{cc}/dt and crystallization rate dM_x/dt to decrease (Figure 6a). To maintain a steady state magma chamber under these conditions requires eruption rate dM_e/dt to increase. If, on the other hand, we attempt to reproduce the geochemical trends by allowing crustal assimilation rate to increase, the recharge rate must increase at a much faster rate to compensate for the effects of assimilation (Figure 6b). In this scenario, steady state is only maintained if eruption rates are high, and as a consequence, in order to return the magma chamber to primitive values, higher magma chamber turnover rates are also required. However, an increasing eruption rate seems at odds with the fact that eruption died just as the magma was becoming more primitive. Thus, the most plausible steady state scenario is that shown in Figure 6a, wherein crystallization rates and crustal assimilation rates decrease during recharge.

5.2.3. Summary: Decreasing Assimilation and Crystallization is Required During Recharge

Based on the above analysis, the increasing primitiveness and decreasing crustal component require recharge with a primitive magma and a decrease in the rates of crustal assimilation and fractional crystallization relative to recharge rate. We also showed that assimilation and fractional crystallization alone cannot explain this trend, and eruption has no effect other than slowing down the rate of geochemical evolution for a given recharge rate. While our analysis cannot distinguish between steady state or nonsteady state magma chambers, the requirement for decreasing crustal assimilation relative to recharge may not be intuitive given that the addition of more magmas should gradually heat up the country rock, making it easier to assimilate. We will return to this problem later, but to evaluate whether the magmatic recharge

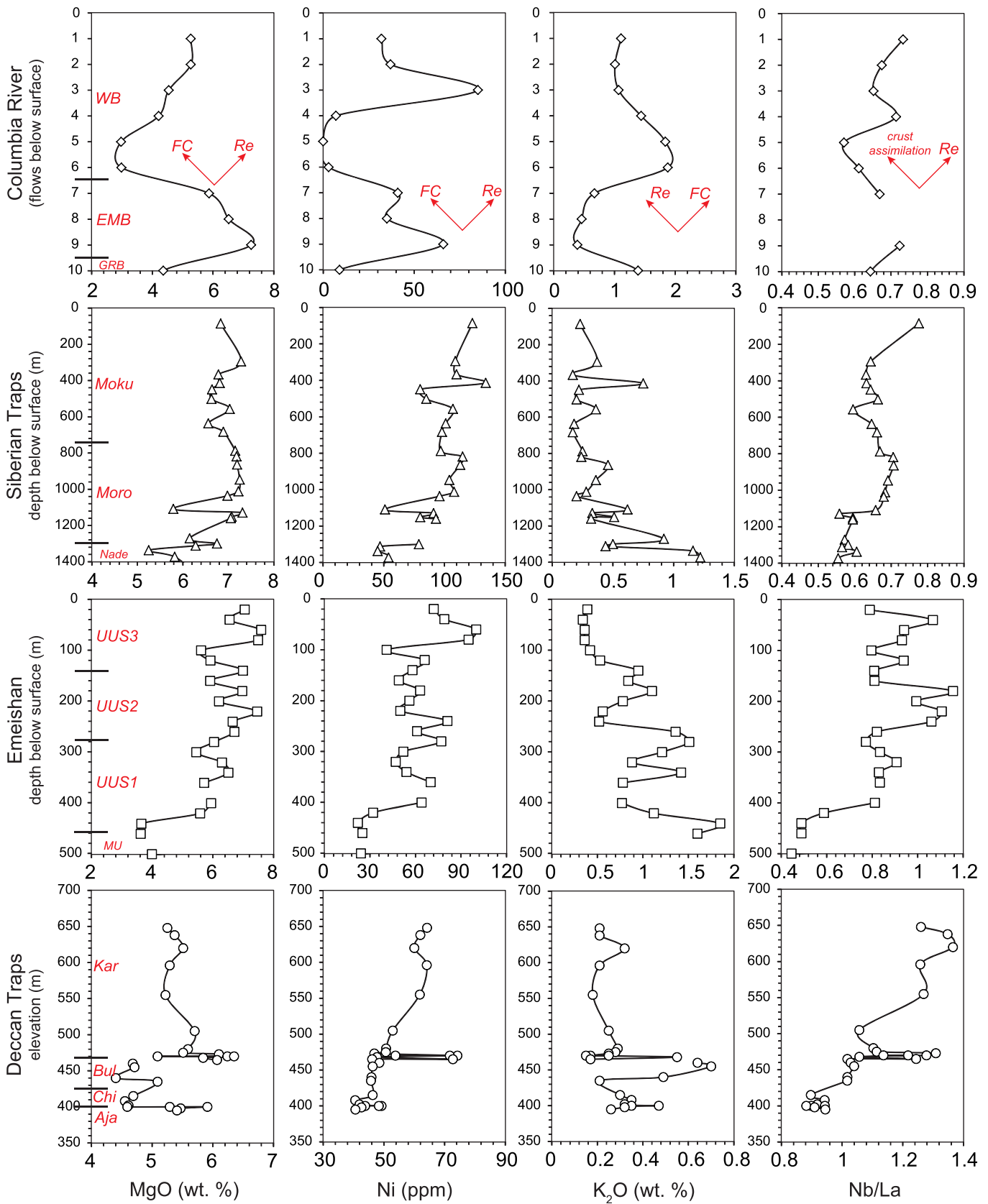


Figure 7.

processes studied here are more general, we examine the volcanic stratigraphy of other large igneous provinces.

5.3. Magmatic Recharge in Large Igneous Basalt Provinces

To evaluate whether the trends toward increasing primitiveness seen in our study might be a general feature, we examined flow sequences from the Columbia River (USA), Siberian Traps, Emeishan, and Deccan Traps flood basalts. Data were compiled from the Georoc database (<http://georoc.mpch-mainz.gwdg.de/georoc/>) [Beane *et al.*, 1986; Hooper, 2000; Lightfoot *et al.*, 1990; Peng *et al.*, 1994; Song *et al.*, 2006].

5.3.1. Columbia River Flood Basalt

The Columbia River Basalt is a Cenozoic continental flood basalt province that covers approximately 200,000 km² in southeastern Washington, northeastern Oregon, and western Idaho (USA). It has been divided into five flow intervals, the Saddle Mountain, Wanapum, Eckler Mountain, Grande Ronde, and Imnaha basalt flows, where the last four formations were erupted within two Myr [e.g., Beeson *et al.*, 1985; Hooper, 2000; Swanson *et al.*, 1979]. Here we selected continuous lava flow profiles containing the Wanapum, and Eckler Mountain formations. Details about the profiles are found in Hooper and Hawkesworth [1993]. Compiled geochemical data are shown in Figure 7, where there are clear segments in which MgO and Ni increase, K₂O decreases, and Nb/La increases up section, indicating the presence of segments with increasing primitiveness with time. AFC processes are thought to have been important in the formation of the Columbia River basalts [Carlson *et al.*, 1981; Ramos *et al.*, 2005; Wolff *et al.*, 2008]. Our observations suggest that several magmatic recharge pulses may have been involved.

5.3.2. Siberian Traps Flood Basalt

The Permian-Triassic Siberian Traps erupted within a period of 1 Myr around 250 Ma [Sharma, 1997]. Siberian Traps can be divided broadly into four volcanic sequences [Fedorenko *et al.*, 1996; Sharma *et al.*, 1991; Sharma, 1997]: Putorana, Noril'sk, Maimecha-Kotui, and Nizhnyaya Tunguska. The Noril'sk represents the main volcanic profile in the Siberian Traps and can be divided into 11 suites. We selected the top three suites with continuous profiles from the Noril'sk sequence [Lightfoot *et al.*, 1990]. It can be seen that the Noril'sk sequence becomes slightly more primitive up section (increasing Ni and decreasing K₂O), consistent with the phenomena observed in our study (Figure 7). Indeed, previous studies have already reported the role of AFC and recharge in formation of these basalts [e.g., Lightfoot *et al.*, 1990; Sharma *et al.*, 1991; Sharma, 1997].

5.3.3. Emeishan Flood Basalt

The Emeishan Large Igneous Province covers large areas in southwest China and northern Vietnam, and was erupted within two million years around 260 Ma [Ali *et al.*, 2005; Guo *et al.*, 2004; Zhou *et al.*, 2006]. The main outcrop occupies about 2.5×10^5 km². Individual volcanic sections may vary considerably across the province. We selected a ~1000 m thick basaltic sequence from the Yangliuping region in the northern part of the Emeishan basalt province; this sequence can be divided into lower, middle, and upper units, the latter of which can be further subdivided into three subunits [Song *et al.*, 2006]. Here we show continuous profiles from the upper units in Figure 7. Ni and Nb/La initially decrease up section, but then increase. K₂O increases initially and then decreases, consistent with magmatic recharge. Previous studies have mentioned the importance of AFC processes [Song *et al.*, 2006], but the trend toward increasing primitiveness seems to also require recharge.

5.3.4. Deccan Traps Flood Basalt

The Deccan traps erupted predominantly on the Indian shield at ~65 Ma. The new uranium-lead (U-Pb) zircon geochronology of Deccan rocks showed that the main phase of eruptions was accomplished within one Myr [Schoene *et al.*, 2015]. A comprehensive stratigraphic framework for the Deccan basalts was provided by Beane *et al.* [1986] based on studies in the Western Ghats. Three major subgroups and 11 formations have been identified. The lower six formations suggest the importance of AFC processes

Figure 7. Plots of MgO, Ni, K₂O, and Nb/La for profiles from Columbia River basalt, Siberian Traps, Emeishan, and Deccan Traps (data compiled from <http://georoc.mpch-mainz.gwdg.de/georoc/>). Columbia River basalt includes Eckler Mountain Basalt (EMB) and Wanapum Basalt (WB) flows, following the stratigraphic nomenclature of Hopper [2000]. The Siberian Traps profile can be divided into three formations from bottom to top: Nadezhdinsky (Nade), Morongovsky (Moro), and Mokulaevky (Moku), following the work of Lightfoot *et al.* [1990]. For the Emeishan large igneous province, the Yangliuping basaltic sequence was selected; it is divided into five units [Song *et al.*, 2006], and only the top three units are selected. For the Deccan Traps, we examine the semicontinuous section from Kumar *et al.* [2010]: Ajanta (Aja), Chikhli (Chi), Buldhana (Bul), and Karanja (Kar) formations are included.

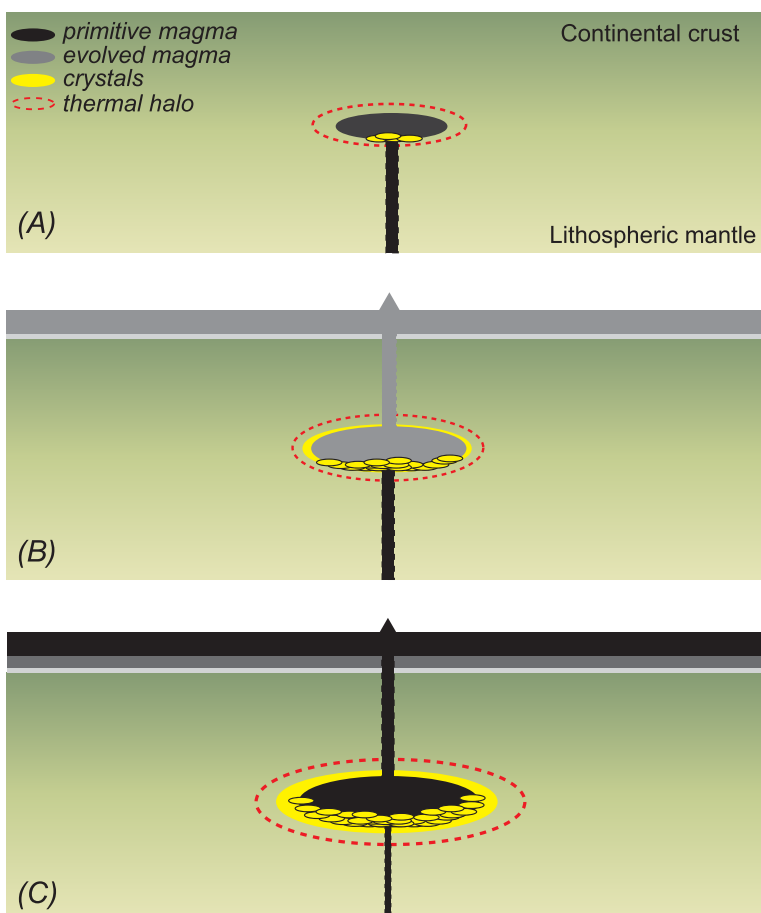


Figure 8. Cartoons describing the effect of recharge on reverse evolution trend for flood basalts. (a) Cooling stage: primitive magma intrudes into the cold crust, causing it to undergo fractional crystallization and assimilate the wall rock. (b) Continuous recharge of primitive magma expands the thermal halo of the wall rock, but progressive crystallization of cumulates around the magma chamber suppresses crustal assimilation. (c) Magma chamber becomes more primitive with progressive recharge, but thermal weakening of country rock prevents over-pressures from building up, resulting in a decline of eruption rates.

[Kumar *et al.*, 2010; Peng *et al.*, 1994], while the upper four formations suggest the role of recharge [Cox and Hawkesworth, 1984; Devey and Cox, 1987]. In this paper, we show a small semicontinuous extrusive section from the eastern Deccan Volcanic Province (DVP) [Kumar *et al.*, 2010]. Layered basalts from four formations, Ajanta, Chikhli, Buldhana, and Karanja, are shown in Figure 7. It can be seen that the basalt sequence becomes slightly more primitive up section.

5.4. Toward a General Model for Magmatic Recharge in Continental Flood Basalt

We find that trends toward increasing primitiveness with time may be a common feature of continental flood basalts, suggesting that magmatic recharge and decreasing relative crustal assimilation rates are important in the evolution of the magma chambers that feed flood basalts. We note that the Chifeng flood basalt is much smaller (more than an order of magnitude) than the Columbia, Deccan, Siberian, and Emeishan flood basalts, which indicates that recharge operates at many scales.

There are a number of ways that magmas can become more primitive with time. One possibility is that with progressive recharge, the magma chamber reaches thermal and compositional steady state because the country rock has become warmer, decreasing the cooling rates and hence crystallization rates of the magma body [Annen *et al.*, 2006]. However, one might expect that, as the surrounding wall rock warms up, crustal assimilation would become more efficient because it would be easier to melt the wall rock. Indeed, theoretical studies suggest that magma chambers undergoing continuous recharge but limited eruption (smaller than recharge rate) can potentially assimilate more than 50% wall rock, depending on the composition of the wall rock and the temperature of the magma chamber [Karlstrom *et al.*, 2010]. What limits the

eruption rate is unclear, but with prolonged residence of the magma chamber, the warming wall rock will weaken, decreasing the rate at which overpressures in the magma chamber can build up [Jellinek and DePaolo, 2003].

We offer another possibility. During the initiation of a magma chamber, these early magmas cool and differentiate, generating a thickening rind of cumulates along the margins of the magma body. If the cumulate chemical boundary layer is nonconvecting, the characteristic lengthscale through which heat must diffuse into the country rock progressively increases, slowing down cooling. Continued recharge advects heat into the system, gradually heating up and weakening the wall rock. This may allow the magma chamber to expand, but because of the thickening cumulate rind, crustal assimilation may become limited (Figure 8). Consequently, the magma chamber becomes progressively more primitive in composition. While this is happening, some amount of magmas erupt, providing a record of the secular evolution of the magma chamber. Importantly, recharging magma chambers could result in the formation of homogeneous, primitive magma bodies.

6. Conclusions

The Baichahe vertical section from the Chifeng flood basalt is represented by initial eruption of evolved basalts followed by increasing primitiveness with time. This trend toward increasing primitiveness cannot be explained by standard assimilation-fractional crystallization (AFC) processes alone and instead requires recharge of a primitive magma. In particular, we show that initial emplacement of primitive magmas into the cold crust results in crystallization and crustal assimilation, but that subsequent mafic recharge returns the magma body to more primitive and hotter conditions. We show trends toward increasing primitiveness seen in the Chifeng flood basalt series is also seen in many other flood basalts, suggesting that flood basalts tap deep crustal magma chambers, undergoing recharge.

Acknowledgments

This study was supported by NSFC (grant 41172060), and SKLMDR (grant ZZKT-201307). All geochemical data are available in the paper and upon request to the corresponding author. We are grateful to Wei Pu, Ye Liu, and Tao Yang for their technical support in the laboratory. Fu-Gen Mao and Zhen-Chao Wang attended the field investigations of this study. Thanks to Monica Erdman, Michael Farner, and He-He Jiang for discussions during this work. The author is grateful for financial support from the China Scholarship Council. We greatly appreciate the thorough reviews and helpful comments from Tyrone Rooney and Esteban Gazel.

References

- Ali, J. R., G. M. Thompson, M. F. Zhou, and X. Song (2005), Emeishan large igneous province, SW China, *Lithos*, *79*, 475–489, doi:10.1016/j.lithos.2004.09.013.
- Anderson, D. L. (1994), The sublithospheric mantle as the source of continental flood basalts; the case against the continental lithosphere and plume head reservoirs, *Earth Planet. Sci. Lett.*, *123*, 1–3, doi:10.1016/0012-821X(94)90273-9.
- Annen, C., J. D. Blundy, and R. S. J. Sparks (2006), The genesis of intermediate and silicic magmas in deep crustal hot zones, *J. Petrol.*, *47*, 505–539, doi:10.1093/ptrology/egi084.
- Arndt, N. T., G. K. Czamanske, J. L. Wooden, and V. A. Fedorenko (1993), Mantle and crustal contributions to continental flood volcanism, *Tectonophysics*, *223*, 39–52, doi:10.1016/0040-1951(93)90156-E.
- Beane, J., C. A. Turner, P. R. Hooper, K. V. Subbarao, and J. N. Walsh (1986), Stratigraphy, composition and form of the Deccan basalts, Western Ghats, India, *Bull. Volcanol.*, *48*, 61–83, doi:10.1007/BF01073513.
- Beeson, M. H., K. R. Fecht, S. Reidel, and T. Tolan (1985), Regional correlations within the Frenchman Springs Member of the Columbia River Basalt Group: New insights into the middle Miocene tectonics of northwestern Oregon, *Oreg. Geol.*, *47*, 87–96.
- Carlson, R. W., G. W. Lugmair, and J. D. Macdougall (1981), Columbia River volcanism: The question of mantle heterogeneity or crustal contamination, *Geochim. Cosmochim. Acta*, *45*, 2483–2499, doi:10.1016/0016-7037(81)90100-9.
- Chen, X. Y., L. H. Chen, Y. Chen, G. Zeng, and J. Q. Liu (2014), Distribution summary of Cenozoic basalts in Central and Eastern China [in Chinese with English abstract], *Geol. J. China Univ.*, *20*, 507–519.
- Cox, K. G., and C. J. Hawkesworth (1984), Relative contribution of crust and mantle to flood basalt magmatism, Mahabaleshwar area, Deccan Traps, *Philos. Trans. R. Soc. London A*, *310*, 627–641, doi:10.1098/rsta.1984.0011.
- DePaolo, D. J. (1981), Trace element and isotopic effects of combined wallrock assimilation and fractional crystallization, *Earth Planet. Sci. Lett.*, *53*, 189–202, doi:10.1016/0012-821X(81)90153-9.
- Devey, C. W., and K. G. Cox (1987), Relationships between crustal contamination and crystallisation in continental flood basalt magmas with special reference to the Deccan Traps of the Western Ghats, India, *Earth Planet. Sci. Lett.*, *84*, 59–68, doi:10.1016/0012-821X(87)90176-2.
- Fedorenko, V. A., P. C. Lightfoot, A. J. Naldrett, G. K. Czamanske, C. J. Hawkesworth, J. L. Wooden, and D. S. Ebel (1996), Petrogenesis of the flood-basalt sequence at Noril'sk, north central Siberia, *Int. Geol. Rev.*, *38*, 99–135, doi:10.1080/00206819709465327.
- Gao, S., T. C. Luo, B. R. Zhang, H. F. Zhang, Y. W. Han, Z. D. Zhao, and Y. K. Hu (1998), Chemical composition of the continental crust as revealed by studies in East China, *Geochim. Cosmochim. Acta*, *62*, 1959–1975, doi:10.1016/S0016-7037(98)00121-5.
- Gast, P. W. (1968), Trace element fractionation and the origin of tholeiitic and alkaline magma types, *Geochim. Cosmochim. Acta*, *32*, 1057–1086, doi:10.1016/0016-7037(68)90108-7.
- Govindaraju, G. (1994), Compilation of working values and sample description for 383 geostandards, *Geostand. Newsl.*, *18*, 1–158.
- Guo, F., W. Fan, Y. Wang, and C. Li (2004), When did the Emeishan mantle plume activity start? Geochronological and geochemical evidence from ultramafic-mafic dikes in southwestern China, *Int. Geol. Rev.*, *46*, 226–234, doi:10.2747/0020-6814.46.3.226.
- Han, B. F., S. G. Wang, and H. Kagami (1999), Trace element and Nd-Sr isotope constraints on origin of the Chifeng flood basalts, North China, *Chem. Geol.*, *155*, 187–199, doi:10.1016/S0009-2541(98)00172-7.
- Ho, K. S., Y. Liu, J. C. Chen, and H. J. Yang (2008), Elemental and Sr-Nd-Pb isotopic compositions of late Cenozoic Abaga basalts, Inner Mongolia: Implications for petrogenesis and mantle process, *Geochem. J.*, *42*, 339–357.

- Hong, L. B., Y. H. Zhang, S. P. Qian, J. Q. Liu, Z. Y. Ren, and Y. G. Xu (2013), Constraints from melt inclusions and their host olivines on the petrogenesis of Oligocene-Early Miocene Xindian basalts, Chifeng area, North China Craton, *Contrib. Mineral. Petrol.*, *165*, 305–326, doi:10.1007/s00410-012-0810-0.
- Hooper, P. R. (2000), Chemical discrimination of Columbia River basalt flows, *Geochem. Geophys. Geosyst.*, *1*(6), 1024, doi:10.1029/2000GC00040.
- Hooper, P. R., and C. J. Hawkesworth (1993), Isotopic and geochemical constraints on the origin and evolution of the Columbia River basalt, *J. Petrol.*, *34*, 1203–1246, doi:10.1093/petrology/34.6.1203.
- Hu, S. B., P. B. O'Sullivan, A. Raza, and B. P. Kohn (2001), Thermal history and tectonic subsidence of the Bohai Basin, northern China: A Cenozoic rifted and local pull-apart basin, *Phys. Earth Planet. Inter.*, *126*, 221–235, doi:10.1016/S0031-9201(01)00257-6.
- Jellinek, A. M., and D. J. DePaolo (2003), A model for the origin of large silicic magma chambers: Precursors of caldera-forming eruptions, *Bull. Volcanol.*, *65*, 363–381, doi:10.1007/s00445-003-0277-y.
- Jia, W., H. Z. Zhu, and J. A. Shao (2002), Temporal-spatial distribution of Cenozoic basalts in Chifeng area, Inner Mongolia [in Chinese], *Geol. Rev.*, *48*, 267–272.
- Karlstrom, L., J. Dufek, and M. Manga (2010), Magma chamber stability in arc and continental crust, *J. Volcanol. Geotherm. Res.*, *190*, 249–270, doi:10.1016/j.jvolgeores.2009.10.003.
- King, S. D., and D. L. Anderson (1995), An alternative mechanism of flood basalt formation, *Earth Planet. Sci. Lett.*, *136*, 269–279, doi:10.1016/0012-821X(95)00205-Q.
- Kumar, K. V., C. Chavan, S. Sawant, K. N. Raju, P. Kanakdande, S. Patode, K. Deshpande, S. Krishnamacharyulu, T. Vaideswaran, and V. Balaram (2010), Geochemical investigation of a semi-continuous extrusive basaltic section from the Deccan Volcanic Province, India: Implications for the mantle and magma chamber processes, *Contrib. Mineral. Petrol.*, *159*, 839–862, doi:10.1007/s00410-009-0458-6.
- Kuritani, T., and E. Nakamura (2002), Precise isotope analysis of nanogram-level Pb for natural rock samples without use of double spikes, *Chem. Geol.*, *186*, 31–43, doi:10.1016/S0009-2541(02)00004-9.
- Lassiter, J., D. DePaolo, and J. Mahoney (1995), Geochemistry of the Wrangellia flood basalt province: Implications for the role of continental and oceanic lithosphere in flood basalt genesis, *J. Petrol.*, *36*, 983–1009, doi:10.1093/petrology/36.4.983.
- Lassiter, J. C., and D. J. DePaolo (1997), Plume/lithosphere interaction in the generation of continental and oceanic flood basalts: Chemical and isotopic constraints, in *Large Igneous Provinces: Continental, Oceanic, and Planetary Flood Volcanism*, vol. 100, edited by J. J. Mahoney and M. F. Coffin, pp. 335–355, AGU, Washington, D. C., doi:10.1029/GM100p0335.
- Lee, C.-T. A., and E. J. Chin (2014), Calculating melting temperatures and pressures of peridotite protoliths: Implications for the origin of cratonic mantle, *Earth Planet. Sci. Lett.*, *403*, 273–286, doi:10.1016/j.epsl.2014.06.048.
- Lee, C.-T. A., T. C. Lee, and C. T. Wu (2014), Modeling the compositional evolution of recharging, evacuating, and fractionating (REFC) magma chambers: Implications for differentiation of arc magmas, *Geochim. Cosmochim. Acta*, *143*, 8–22, doi:10.1016/j.gca.2013.08.009.
- Lightfoot, P., and C. Hawkesworth (1988), Origin of Deccan Trap lavas: Evidence from combined trace element and Sr-, Nd- and Pb-isotope studies, *Earth Planet. Sci. Lett.*, *91*, 89–104, doi:10.1016/0012-821X(88)90153-7.
- Lightfoot, P. C., A. Naldrett, N. Gorbachev, W. Doherty, and V. A. Fedorenko (1990), Geochemistry of the Siberian Trap of the Noril'sk area, USSR, with implications for the relative contributions of crust and mantle to flood basalt magmatism, *Contrib. Mineral. Petrol.*, *104*, 631–644, doi:10.1007/BF01167284.
- Liu, R. X., W. J. Chen, J. Z. Sun, and D. M. Li (1992), The K-Ar age and tectonic environment of Cenozoic volcanic rock in China, in *The Age and Geochemistry of Cenozoic Volcanic Rock in China* [in Chinese], edited by R. X. Liu, pp. 1–43, Seismol. Press, Beijing.
- Liu, Y., S. Gao, H. Yuan, L. Zhou, X. Liu, X. Wang, Z. Hu, and L. Wang (2004), U-Pb zircon ages and Nd, Sr, and Pb isotopes of lower crustal xenoliths from North China Craton: Insights on evolution of lower continental crust, *Chem. Geol.*, *211*, 87–109, doi:10.1016/j.chemgeo.2004.06.023.
- McDonough, W. F., and S. S. Sun (1995), The composition of the Earth, *Chem. Geol.*, *120*, 223–253, doi:10.1016/0009-2541(94)00140-4.
- McKenzie, D., and R. K. O'Nions (1991), Partial melt distributions from inversion of rare Earth element concentrations, *J. Petrol.*, *32*, 1021–1091, doi:10.1093/petrology/32.5.1021.
- O'Neill, H. S. C., and F. Jenner (2012), The global pattern of trace element distributions in ocean floor basalts, *Nature*, *491*, 698–705.
- Peng, Z. X., J. J. Mahoney, P. Hooper, C. Harris, and J. Beane (1994), A role for lower continental crust in flood basalt genesis? Isotopic and incompatible element study of the lower six formations of the western Deccan Traps, *Geochim. Cosmochim. Acta*, *58*, 267–288, doi:10.1016/0016-7037(94)90464-2.
- Ramos, F. C., J. A. Wolff, and D. L. Tollstrup (2005), Sr isotope disequilibrium in Columbia River flood basalts: Evidence for rapid shallow-level open-system processes, *Geology*, *33*, 457–460, doi:10.1130/G21512.1.
- Schoene, B., K. M. Samperton, M. P. Eddy, G. Keller, T. Adatte, S. A. Bowring, S. F. R. Khadri, and B. Gertsch (2015), U-Pb geochronology of the Deccan Traps and relation to the end-Cretaceous mass extinction, *Science*, *347*, 182–184, doi:10.1126/science.Aaa0118.
- Sharma, M. (1997), Siberian traps, in *Large Igneous Provinces: Continental, Oceanic, and Planetary Flood Volcanism*, *Geophys. Monogr.*, vol. 100, edited by J. J. Mahoney and M. F. Coffin, pp. 273–295, AGU, Washington, D. C.
- Sharma, M., A. R. Basu, and G. Nesterenko (1991), Nd-Sr isotopes, petrochemistry, and origin of the Siberian flood basalts, USSR, *Geochim. Cosmochim. Acta*, *55*, 1183–1192, doi:10.1016/0016-7037(91)90177-7.
- Shaw, D. M. (1970), Trace element fractionation during anatexis, *Geochim. Cosmochim. Acta*, *34*, 237–243, doi:10.1016/0016-7037(70)90009-8.
- Silver, P. G., M. D. Behn, K. Kelley, M. Schmitz, and B. Savage (2006), Understanding cratonic flood basalts, *Earth Planet. Sci. Lett.*, *245*, 190–201, doi:10.1016/j.epsl.2006.01.050.
- Song, X. Y., M. F. Zhou, R. R. Keays, Z. M. Cao, M. Sun, and L. Qi (2006), Geochemistry of the Emeishan flood basalts at Yangliuping, Sichuan, SW China: Implications for sulfide segregation, *Contrib. Mineral. Petrol.*, *152*, 53–74, doi:10.1007/s00410-006-0094-3.
- Spera, F. J., and W. A. Bohrson (2001), Energy-constrained open-system magmatic processes. I: General model and energy-constrained assimilation and fractional crystallization (EC-AFC) formulation, *J. Petrol.*, *42*, 999–1018, doi:10.1093/petrology/42.5.999.
- Spera, F. J., and W. A. Bohrson (2002), Energy-constrained open-system magmatic processes. 3: Energy-Constrained Recharge, Assimilation, and Fractional Crystallization (EC-RAFC), *Geochem. Geophys. Geosyst.*, *3*(12), 8001, doi:10.1029/2002GC000315.
- Spera, F. J., and W. A. Bohrson (2004), Open-system magma chamber evolution: An energy-constrained geochemical model incorporating the effects of concurrent Eruption, Recharge, variable Assimilation and Fractional Crystallization (EC-ERA_xFC), *J. Petrol.*, *45*, 2459–2480, doi:10.1093/petrology/egh072.
- Swanson, D. A., T. L. Wright, P. R. Hooper, and R. D. Bentley (1979), Revisions in stratigraphic nomenclature of the Columbia River Basalt Group, *U.S. Geol. Surv. Bull.*, *1457G*, G1–G59.
- White, R. S., and D. McKenzie (1995), Mantle plumes and flood basalts, *J. Geophys. Res.*, *100*, 17,543–17,585, doi:10.1029/95JB01585.

- White, W. M., F. Albarède, and P. Télouk (2000), High-precision analysis of Pb isotope ratios by multi-collector ICP-MS, *Chem. Geol.*, *167*, 257–270, doi:10.1016/S0009-2541(99)00182-5.
- Wolff, J. A., F. C. Ramos, G. L. Hart, J. D. Patterson, and A. D. Brandon (2008), Columbia River flood basalts from a centralized crustal magmatic system, *Nat. Geosci.*, *1*, 177–180, doi:10.1038/ngeo124.
- Wooden, J. L., G. K. Czamanske, V. A. Fedorenko, N. T. Arndt, C. Chauvel, R. M. Bouse, B. S. W. King, R. J. Knight, and D. F. Siems (1993), Isotopic and trace-element constraints on mantle and crustal contributions to Siberian continental flood basalts, Noril'sk area, Siberia, *Geochim. Cosmochim. Acta*, *57*, 3677–3704, doi:10.1016/0016-7037(93)90149-Q.
- Zhou, M. F., J. H. Zhao, L. Qi, W. Su, and R. Hu (2006), Zircon U-Pb geochronology and elemental and Sr-Nd isotope geochemistry of Permian mafic rocks in the Funing area, SW China, *Contrib. Mineral. Petrol.*, *151*, 1–19, doi:10.1007/s00410-005-0030-y.